

Overview of the hypernuclear production in heavy-ion collision experiments

Christophe Rappold

GSI Helmholtz Centre for Heavy Ion Research - Darmstadt, Germany & Universidad de Castilla-La Mancha, Institute of Mathematics applied to Science and Engineering - Ciudad Real, Spain

E-mail: c.rappold@gsi.de

Abstract.

In the last decade, heavy-ion collision experiments have brought new insight to the study of hypernucleus. Experiments using ion induced reactions for hypernuclear research focus on two distinct aspects: the spectroscopy and probing the nuclear reaction. In the case of the experimental spectroscopy, the internal structure of hypernuclei is investigated in order to determine the baryon-baryon interaction in the strangeness sector for the hyper-matter equation of state. The dynamical aspect of the nucleus-nucleus reaction can also be explored by studying the production of hypernuclei. The experimental observations of the production mechanisms responsible for the formation of the hypernuclei in ion collisions will be presented. Depending of the center-of-mass energy and the type of experiment, fixed target or collider, hypernuclei can be produced in the mid-rapidity and/or in the spectator regions. The experimental results from both cases will be presented and discussed.

1. Introduction

The hypernucleus, a bound state of ordinary nucleons and hyperons, has been a subject of research for the understanding of the baryon-baryon interaction in an unified way. The main purpose is to tackle the problem of the neutron stars or the equation of state of baryonic matter up to the strangeness sector. The baryon-baryon interaction could be easily extracted from the hyperon-nucleon and hyperon-hyperon scattering data; however the scarce data sets from the hyperon-nucleon scattering experiments and the impossibility to have hyperon-hyperon scattering experiments have made the direct determination of the baryon-baryon interaction strength within $SU(3)_f$ extremely difficult. By performing precise spectroscopy of Λ -hypernuclear bound states, interaction strength of Λ -N has been deduced indirectly by means of the experimental data and theoretical models [1, 2, 3, 4, 5, 6]. Those spectroscopy experiments have been performed mainly by means of secondary meson beams via (π, K) , (K, π) , or (K^-, K^+) elementary reactions or by means of e^- primary beam via $(e^-, e'^- K^+)$ photoelectric production on fixed target [7]. Additionally to those experimental approaches, hypernuclear production by heavy-ion induced reaction has been theoretically investigated and predicted in 1973 [8]. This first theoretical prospect has led to new experimental approaches for the spectroscopic study of hypernuclei. Indeed, heavy-ion induced reaction on fixed targets and heavy-ion collision in colliders have been performed in the most recent years. It has renewed interest in the production of hypernuclei in central collisions in which those hypernuclear bound



states could be used as a probe to the possible phase transition or the presence of quark-gluon plasma.

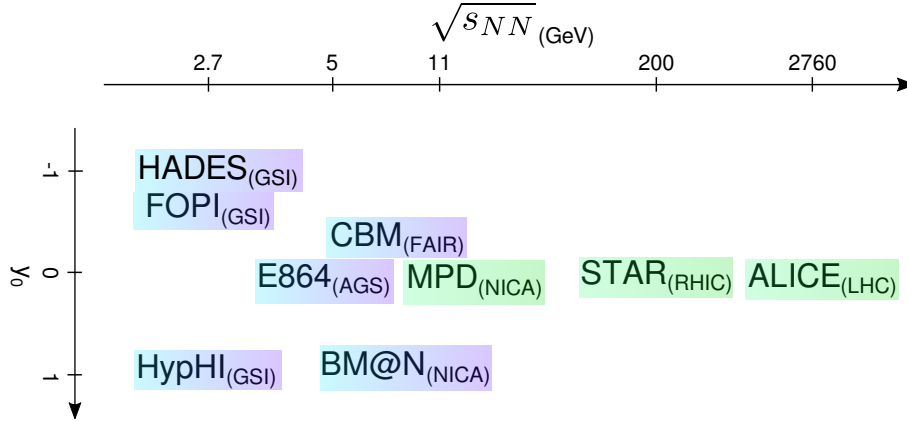


Figure 1. heavy-ion experiments with their respective facility where hypernuclear production have been studied during the last decades.

Figure 1 shows the past, current and future experiments that have published results on the hypernuclear production or dedicates parts of their research plans to the hypernuclear study. First of all, those experiments are sorted by their experimental apparatus: fixed target (in blue rectangle) or collider mode (in green rectangle). Then those experiments are distributed as a function of y_0 and $\sqrt{s_{NN}}$, the rapidity in center-of-mass system region of hypernuclear observations and the center-of-mass energy of the reactions. The discrete repartition between the observed rapidity regions (central or peripheral collisions) and the collision energy has concrete consequences on the physical phenomenon of the hypernuclear production that will be presented in the following sections. Besides experiments that have heretofore been published or reported study of hypernuclei, namely ALICE [9], STAR [10], E864 [11], HADES [12], FOPI [13, 14] and HypHI [15, 16], the NICA and FAIR facilities will host novel experiments (CBM [17], BM@N [18], and MPD [18]) that have a dedicated hypernuclear physics program.

The experimental observables for describing the hypernuclear production mechanism in heavy-ion experiments are mainly the yields, cross sections and multiplicities of the observed hypernuclei. Most of them are reported either as an absolute value or within the experimental acceptance. Those observables can also be determined as a function of the rapidity y_0 or/and the transverse momentum P_t . Those primal observables are essential when compared to theoretical models of the dynamics of the reaction, such as transport models. Additionally, yield ratios to the hyperon yield or to the nuclear yield, such as ${}^3_\Lambda\text{H}/\Lambda$ or ${}^3_\Lambda\text{H}/{}^3\text{He}$ are useful to describe sensitive aspect of the dynamics, and can be more easily extracted from the experimental data, where the efficiency corrections can be canceled out. A double ratio, $S_3 = {}^3_\Lambda\text{H}/{}^3\text{He} \cdot p/\Lambda$ or $S_4 = {}^4_\Lambda\text{H}/{}^4\text{He} \cdot p/\Lambda$, has been introduced by the E864 collaboration [11]; afterwards it was used by the other STAR and ALICE collider experiments to describe possible phase transition and the QGP formation [19]. Those experimental observables will be the presented in the following sections.

2. Ultra-relativistic energy regime

The STAR experiment has been the first to show evidences of the observation of the hypertriton, ${}^3_\Lambda\text{H}$, and the anti-hypertriton hypernuclei in Au-Au collisions at $\sqrt{s_{NN}}=200$ GeV in the ultra-relativistic energy regime [10]. Those hypernuclear bound states are considered to be formed at the freeze-out of the quark gluon plasma. The published results presented some

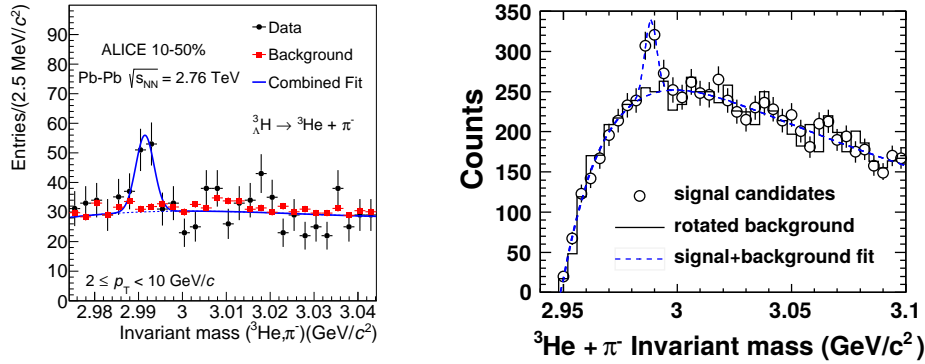


Figure 2. Invariant mass spectrum of the two-body decay reconstruction of ${}^3_{\Lambda}\text{H}$ hypernuclei from the ALICE [9] and STAR experiments [10] in the left and right panel, respectively. Similar invariant mass spectra of anti-hypertriton can be found in the respective references [10, 9].

spectroscopy aspects, such as invariant mass spectrum shown in Figure 2 or its extracted lifetime besides several yield ratios and S_3 factor [10]. It was first claimed that the enhancement of the production of hypertriton at the mid-rapidity would be a signature of the phase transition and formation of the QGP [10] based on theoretical prediction [19]. After the beam scan program of the STAR experiment, additional results on the S_3 factor as a function of the energy in the center-of-mass system have been presented and reported [20]. As well, the ALICE experiment has reported and published the evidence of the hypertriton and anti-hypertriton observation in Pb-Pb collisions at 2.76 TeV [9], shown in Figure 2, with the extracted lifetime and yield ratios [9].

The production mechanism in such collision has been theoretically investigated following the STAR experiment publication and ALICE experiment reports. On one hand, coalescence models through hadronic transport models describe the hypernuclear formation of hyper-cluster at the chemical freeze-out of the QGP phase [19, 21]. On the other hand, thermal models propose a statistical approach to describe the production yield of particle, nucleus, and hypernucleus with their associated anti-particle and bound state at the chemical freeze-out equilibrium, where the entropy per baryon is defined and consequently conserved [22].

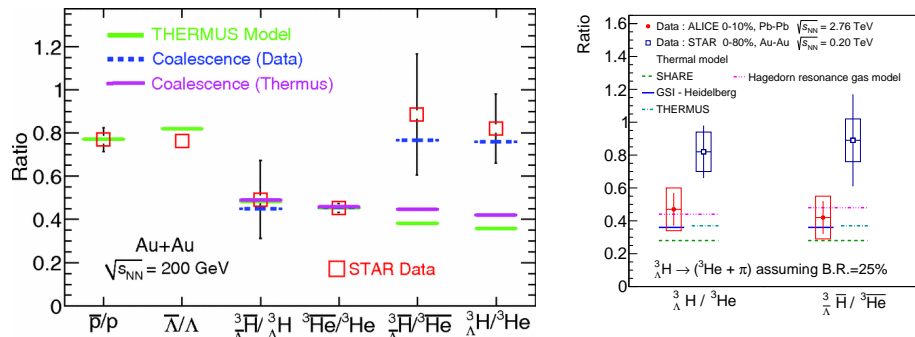


Figure 3. Yield ratios extracted by STAR [23] and ALICE experiment [9] compared to the expected yield estimated by several models.

Several coalescence calculation approaches have been developed [19, 21] and showed similar trends. It is proposed that the S_3 factor could carry the information of the local correlation

between the baryon number and the strangeness, qualitatively similar to the C_{BS} factor [19]. Some theoretical results were compared directly to the published STAR experiment results, as shown in the left panel of Figure 3. In this case, the coalescence model [23] reproduced the yield ratio ${}^3_\Lambda\text{H}/{}^3\text{He}$, while the THERMUS model [24, 25] used for this comparison could not. Additionally, the theoretical estimation of 0.35 ± 0.003 of this yield ratio by the thermal model [22] could not reproduce the STAR experimental results. Considering the ALICE experimental results on the same yield ratio ${}^3_\Lambda\text{H}/{}^3\text{He}$, shown in right panel of Figure 3, the situation seems to favor a good description from the thermal models [22, 21]. Besides those yield ratios, it should be noted the thermal model fit of the production yields [22, 26] reproduces the experimental data fairly well either for STAR or ALICE experimental data within several orders of magnitude difference, and especially the hypertriton and anti-hypertriton yield [22, 26].

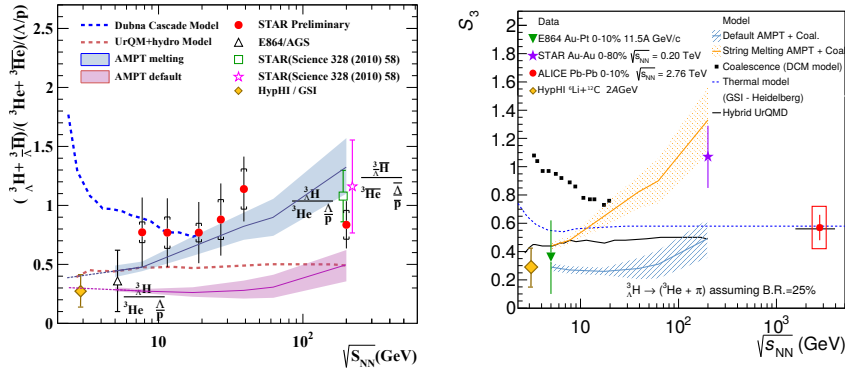


Figure 4. S_3 factor extracted by STAR and ALICE experiments with different model comparisons [20, 9].

The case of the double ratio S_3 is also interesting, since the distinct theoretical approaches for the hypernuclear production in the QGP describe differently the evolution of the S_3 factor. The thermal models predict generally that this double ratio is mostly independent from the energy of the collision [22, 21], while the coalescence models predict different energy dependencies, decreasing or increasing as the beam energy is increased [21, 19]. Figure 4 shows the results from the reported STAR beam energy scan program, the published STAR and ALICE results [10, 20, 9]. The recent S_3 estimation from the HypHI experiment at $\sqrt{s_{NN}} = 2.7$ GeV has been added to those published figures. Several theoretical models are shown and compared to the experimental data available. With the current situation from the preliminary results of STAR beam scan program, an increasing trend is noticeable from the left panel of Figure 4, which is not confirmed by the ALICE experimental results shown in the right panel of Figure 4. The estimation from thermal model [22] reproduces the ALICE results when a feed-down from the contribution of the strong decay of resonances is included, increasing the Λ/p ratio contribution to the S_3 . A similar tendency can be noticed from the second compared thermal model [21]; however, the theoretical calculation within this framework will need to be extended to the beam energy of the ALICE experiment to assure a proper comparison. Contrarily, coalescence model calculations reported an higher S_3 factor and energy dependency. The model [19] predicted a value close to unity which could correspond to the manifestation of the quark deconfinement. The published STAR results have been considered as a first hint as expressed in [10]; however, the recent ALICE results [9] bring new contradictory light onto this possible interpretation of the “AMPT+melting string” model [19].

3. Relativistic energy regime

At a lower center-of-mass energy, several other experiments have already been performed in the past and more recently. With a lower beam energy than in ultra-relativistic regime, experiments have focused on different rapidity regions for the hypernuclear study. The E864 experiment at AGS facility published results of the ${}^3_\Lambda\text{H}$ production yield and upper limit of ${}^4_\Lambda\text{H}$ yield in the central collision of Au beam at 11.5 GeV/c per nucleon on a fixed Pt target [11]. Figure 5 shows the invariant mass spectrum of ${}^3_\Lambda\text{H}$ published by the E864 experiment with a reported ${}^3_\Lambda\text{H}$ signal significance of 2σ [11]. The S_3 double ratio was for the first time extracted and published by the E864 experiment [11]; a value of 0.36 ± 0.26 was reported. This double ratio was introduced initially in order to compare the production of hypernuclei in central collision with the production of ordinary nuclei with a same baryon number A . This comparison would lead to estimate the additional penalty factor required, when a strange baryon is included in the coalescence process. It was notified that there was an extra penalty factor of 3 to produce ${}^3_\Lambda\text{H}$ compared to ${}^3\text{He}$; however, consideration about the smaller binding energy of ${}^3_\Lambda\text{H}$ (around 2.2 MeV) than the one of ${}^3\text{He}$ (8.1 MeV) and the larger size of ${}^3_\Lambda\text{H}$ than ${}^3\text{He}$ may explain the lower production yield of ${}^3_\Lambda\text{H}$ in the central collision. Besides ${}^3_\Lambda\text{H}$, the study of ${}^4_\Lambda\text{H}$ could not be performed completely since the ${}^4_\Lambda\text{H}$ signal was not significant enough. An upper limit at 90% confidence level was then estimated for the ${}^4_\Lambda\text{H}$ production yield and the factor $S_4 = {}^4_\Lambda\text{H}/{}^4\text{He} \cdot p/\Lambda$ [11].

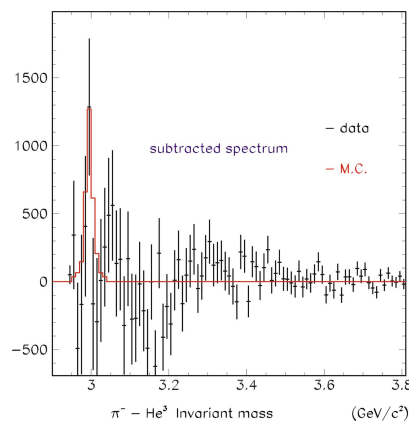


Figure 5. Invariant mass spectrum of the two-body decay reconstruction of hypertriton from E864 experiment [11].

At a lower beam energy, the HADES and FOPI experiments from the GSI facility have conducted hypernuclear study in the target rapidity region. HADES experiment analyzing the reaction $\text{Ar} + \text{KCl}$ at 1.76 AGeV within the range of rapidity y_0 , $[-0.7, 0.1]$, did not observe any ${}^3_\Lambda\text{H}$ signal [12], and reported an upper limit at 99.7% confidence level for the hypertriton production yield and for the ${}^3_\Lambda\text{H}/\Lambda$ yield ratio [12]. The yield ratio ${}^3_\Lambda\text{H}/\Lambda$ was estimated to be inferior to $2.5 \pm 0.3 \times 10^{-2}$ [12]. FOPI experiment has already reported preliminary results of evidence of the observation of ${}^3_\Lambda\text{H}$ and ${}^4_\Lambda\text{H}$ in specific rapidity range y_0 and transverse momentum interval P_t/m , $[-0.56, -0.11] \times [0.2, 0.4]$ and $[-0.67, -0.11] \times [0.15, 0.35]$, respectively [13, 14]. While the preliminary observation of ${}^3_\Lambda\text{H}$ and ${}^4_\Lambda\text{H}$ appeared clear, the comparison between the published upper limit of the yield ratio ${}^3_\Lambda\text{H}/\Lambda$ from HADES experiment within a similar rapidity interval and the estimated yield ratio ${}^3_\Lambda\text{H}/\Lambda$ of 0.52 ± 0.04 casts some incompatibility with the HADES upper limit. Additional considerations for the final FOPI experimental results are pending.

In the projectile fragment rapidity region, hypernuclear study has also been carried out, firstly at LBNL Bevatron with ${}^{16}\text{O}$ beams at 2.1 AGeV on a polyethylene target [27] and then at JINR

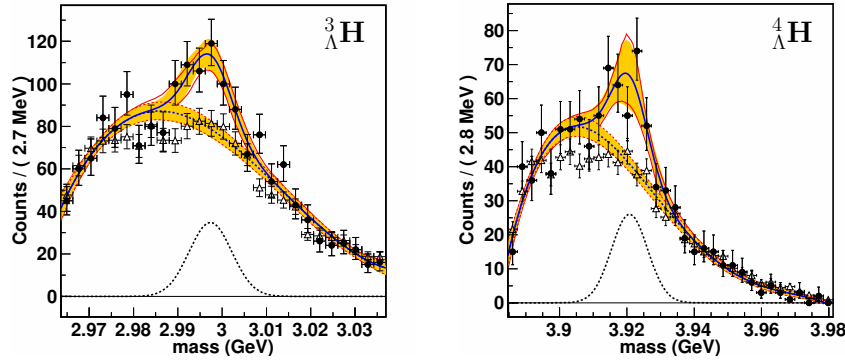


Figure 6. Invariant mass spectrum of two body decay reconstruction of ${}^3_{\Lambda}\text{H}$ and ${}^4_{\Lambda}\text{H}$ of the HypHI experiment in left and right panel respectively [15].

Dubna in the reaction of a beam of ${}^4\text{He}$ at 3.7 A GeV and ${}^7\text{Li}$ at 3.0 A GeV on a polyethylene target [28, 29]. The results on hypernuclear production from those first experiments were not clear enough because of the low statistics acquired and analyzed. More recently, the results from the HypHI experiment on the hypernuclear production have been published [15, 16]. ${}^3_{\Lambda}\text{H}$ and ${}^4_{\Lambda}\text{H}$ hypernuclei were observed in the reaction of ${}^6\text{Li}$ beam at 2 A GeV on a ${}^{12}\text{C}$ fixed target. Figure 6 shows the invariant mass spectrum of observed ${}^3_{\Lambda}\text{H}$ and ${}^4_{\Lambda}\text{H}$ by the HypHI experiment [15]. The ${}^3_{\Lambda}\text{H}$ and ${}^4_{\Lambda}\text{H}$ production cross section of $3.9 \pm 1.4 \mu\text{b}$ and $3.1 \pm 1.0 \mu\text{b}$, and several yield ratios in the projectile rapidity region were extracted and published [16]. For example the ${}^3_{\Lambda}\text{H}/\Lambda$ yield ratio of $2.6 \pm 1.4 \times 10^{-3}$ is compatible with one of the HADES experiment, if we mirror observed rapidity ranges. Additionally, the differential multiplicity as a function of the rapidity and transverse momentum for ${}^3_{\Lambda}\text{H}$ and ${}^4_{\Lambda}\text{H}$ were extracted for the first time and shown in Figure 7. Those published results from HypHI experiment has been compared with theoretical transport model and shows fair agreement with the theoretical calculations [30]. Besides, the S_3 and S_4 double ratio have been estimated to be 0.28 ± 0.14 and 0.08 ± 0.04 . The S_3 value from the HypHI experiment has been added to two published figures of Figure 4 and will help to constrain models in the hadronic phase at lower beam energy.

4. Conclusion

In the ultra-relativistic regime, STAR and ALICE experiments have provided new insights on the hypertriton and anti-hypertriton study [10, 20, 9]. The production aspects have been investigated in details by the ALICE experiment in [9]. Combining results from both experiments shows theoretical models draw different conclusion on the hypertriton formation in the QGP phase. Improvement on the experimental estimations will help to draw clearer conclusion on the model predictions especially on the yield ratios like ${}^3_{\Lambda}\text{H}/{}^3\text{He}$ and the S_3 factor. At lower beam energy, in the relativistic regime, recent results on the projectile rapidity region by the HypHI experiment [15, 16] will help transport models and coalescence models to obtain a more precise description of the reaction mechanism and of the dynamics between the participant and spectator region [21, 31, 32, 33, 34]. Additional experiments, such as the FOPI experiment, are also focusing on the hypernuclear study and will provide further information on the hypernuclear production in the target rapidity region with their final experimental results. In the future, more results from the HypHI experiment are also expected with the analysis of the second experiment ${}^{20}\text{Ne}+{}^{12}\text{C}$ reaction at 2 A GeV. Moreover, the STAR and ALICE experiments are still accumulating new experimental data and will provide more precise estimation in future, and for instance, the ALICE experiment might access the production of ${}^4_{\Lambda}\text{H}$. Besides those running

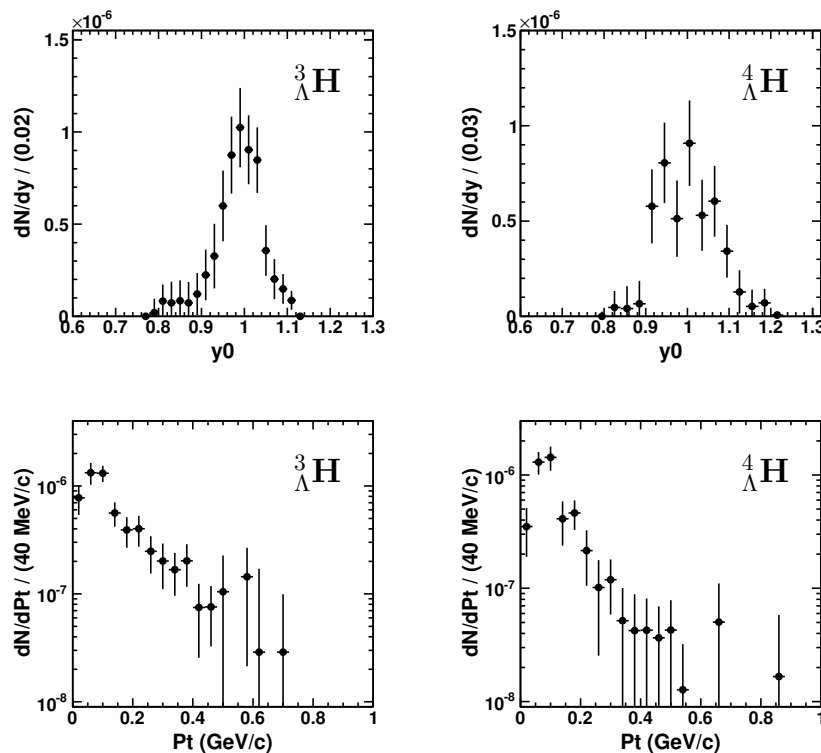


Figure 7. The differential multiplicity as a function of the rapidity y_0 and Pt of extracted ${}^3_{\Lambda}\text{H}$ and ${}^4_{\Lambda}\text{H}$ signal [16].

experiments, new experiments are in preparation within the new FAIR and NICA facilities, which will contribute to the study of the hypernuclear production in heavy-ion reaction.

Acknowledgements

This work has been supported by the HypHI project funded by the Helmholtz association as Helmholtz-University Young Investigators Group VH-NG-239 at GSI, and the German Research Foundation (DFG) under contract number SA 1696/1-1 and EU FP7 Hadron-Physics-2 SPHERE. This work has also been supported by the co-funded program of the University of Castilla-La Mancha “Ayudas para estancias de investigadores invitados en la UCLM para el ao 2015” and FEDER 2014-2020.

References

- [1] Nagels M.M. *et al.* 1977 *Phys. Rev. D* **15** 2547
- [2] Nagels M.M. *et al.* 1979 *Phys. Rev. D* **20** 1633
- [3] Maessen P.M. *et al.* 1989 *Phys. Rev. C* **40** 2226
- [4] Rijken Th.A. and Stokes V.G.J. 1999 *Phys. Rev. C* **59** 21
- [5] Dalitz R.H. and A. Gal A. 1978 *Ann. Phys.* **116** 167
- [6] Millener D.J., Gal A., Dover C.B. and Dalitz R.H. 1985 *Phys. Rev. C* **31** 499
- [7] Hashimoto O. and Tamura H. 2006 *Prog. Part. Nucl. Phys.* **57** 564
- [8] Kerman A. K. and Weiss M. S. 1973 *Phys. Rev. C* **8** 408
- [9] ALICE Collaboration, 2015 *Preprint* arXiv:1506.08453
- [10] STAR Collaboration 2010 *Science* **328** 58
- [11] Armstrong T. A. *et al.* 2004 *Phys. Rev. C* **70** 024902
- [12] HADES Collaboration 2013 *Eur. Phys. J. A* **49** 146
- [13] Y. Zhang, PhD Thesis 2013

- [14] Leifels Y. 2013 *J. Phys.: Conf. Series* **420** 012019
- [15] Rappold C. *et al.* 2013 *Nucl. Phys. A* **913** 170
- [16] Rappold C. *et al.* 2015 *Phys. Lett. B* **747** 129
- [17] Friman B., Hohne C., Knoll J., Leupold S., Randrup J., Rapp R. and Senger P. 2011 *Lect.Notes Phys.* **814** 980
- [18] Kovalenko A.D. *et al.* 2015 *PoS BaldinISHEPPXXII* 002
- [19] Zhang S., Chen J. H., Crawford H., Keane D., Ma Y.G. and Xu Z.B. 2010 *Phys. Lett. B* **684** 224
- [20] Ma Y.G. for STAR collaboration 2014 *EPJ Conf.* **66** 04020
- [21] Steinheimer J., Gudima K. , Botvina A. , Mishustin I., Bleicher M. and Stocker H. 2012 *Phys. Lett. B* **714** 85
- [22] Andronic A., Braun-Munzinger P., Stachel J., and Stocker H. 2011 *Phys. Lett. B* **697** 203
- [23] Cleymans J. *et al.* 2011 *Phys. Rev. C* **84** 054916
- [24] Wheaton S. and Cleymans J. 2005 *J. Phys. G* **31** S1069
- [25] Wheaton S., Cleymans J. and Hauer M. 2009 *Comput. Phys.Commun.* **180** 84
- [26] Elia D. for ALICE Collaboration 2015 *EPJ Conf.* **95** 03008
- [27] Nield K. *et al.*, 1976 *Phys. Rev. C* **13** 1263
- [28] Abdurakhimov A.U. *et al.* 1989 *Nuovo Cimento A* **102** 645
- [29] Avramenko S. *et al.* 1992 *Nucl. Phys. A* **547** 95c
- [30] Le Fevre A. 2015 *these proceedings*
- [31] Gaitanos T., Lenske H. and Mosel U. 2009 *Phys. Lett. B* **675** 297
- [32] Botvina A. S., Mishustin I. N. and Pochodzalla J. 2012 *Phys. Rev. C* **86** 011601
- [33] Topor Pop V. and Das Gupta S. 2010 *Phys. Rev. C* **81** 054911
- [34] Botvina A. S. and Pochodzalla J. 2007 *Phys. Rev. C* **76** 024909